Metmyoglobin-Catalyzed Exogenous and Endogenous Tyrosine Nitration by Nitrite and Hydrogen Peroxide

Stefania Nicolis,[a] Enrico Monzani,[a] Raffaella Roncone,[a] Luca Gianelli,[b] and Luigi Casella*[a]

Abstract: Metmyoglobin catalyzes the nitration of various phenolic compounds in the presence of nitrite and hydrogen peroxide. The reaction rate depends on the reactant concentrations and shows saturation behavior. Two competing paths are responsible for the reaction. In the first, myoglobin reacts according to a peroxidase-like cycle forming two active intermediates, which can induce one-electron oxidation of the substrates. The $MbFe^{IV}=O$ intermediate oxidizes nitrite to nitrogen dioxide, which, after reaction with the phenol or with a phenoxy radical, yields the nitrophenol. In the second mechanism, hydrogen peroxide reacts with iron-bound nitrite to produce an active nitrating species, which we assume to be a protein-bound peroxynitrite species, $MbFe^{III}-N(O)OO$. The high nitrating power of the active species is shown by the fact that the catalytic rate constant is essentially independent of the redox properties of the phenol. The occurrence of one or other of these mechanisms depends on the nitrite concentration: at low $[NO_2^-]$ the nitrating agent is nitrogen dioxide, whereas at high $[NO_2^-]$ the peroxynitrite path is dominant. The myoglobin derivative that accumulates during turnover depends on the mechanism. When the path involving $NO_2^{\bullet}$ is dominant, the spectrum of the $MbFe^{IV}=O$ intermediate is observed. At high nitrite concentration, the Soret band appears at 416 nm, which we attribute to an iron-peroxynitrite species. The $metMb/NO_2^-/H_2O_2$ system competitively nitrates the heme and the endogenous tyrosine at position 146 of the protein. Phenolic substrates protect Tyr146 from nitration by scavenging the active nitrating species. The exposed Tyr103 residue is not nitrated under the same conditions.

Keywords: enzyme catalysis · heme proteins · hydrogen peroxide · myoglobin · nitrogen oxides · peroxynitrite

Introduction

Myoglobin (Mb) is a small monomeric heme protein that is present in high concentration in red muscles.[1] It has been the subject of extensive studies, which have also been performed on Mb site-directed mutants, aimed at gaining information on structure–function relationships of heme proteins in general, as well as at elucidating its actual function(s) in vivo. Mb is usually cited as a protein involved in dioxygen storage and transport in cells,[2] but recently other activities have been found. In particular, the protein is active in oxidative phosphorylation,[3] it shows some peroxidase- and P-450-like catalytic activity,[4] and protects cells against oxidative damage.[5,6] In its reduced form, Mb strongly binds carbon monoxide and nitrogen monoxide,[7,8] whereas in its oxy form it reacts efficiently with nitrogen monoxide to produce a transient intermediate with a bound peroxynitrite moiety.[9,10] Since nitrogen monoxide acts as an inhibitor of cellular respiration through its reaction with cytochrome *c* oxidase, the scavenging effect of Mb for $NO^{\bullet}$ protects the cell from respiratory inhibition.[11,12] The reaction of $NO^{\bullet}$ with oxyMb produces peroxynitrite; there is controversy as to whether bound $ONOO^-$ produced by this reaction is capable of nitrating an endogenous protein Tyr residue under physiological conditions.[10,13] A similar controversy concerns the ability of exogenously supplied peroxynitrite to nitrate proteins, since Bourassa et al.[13] and Witting et al.[14] reported that metMb (from horse heart and human source, respectively) is nitrated at Tyr103 leaving Tyr146 unaffected, whilst Herold et al. reported no significant nitration with metMb and the formation of nitro-Tyr146 with apoMb from horse heart.[15] On the other hand, in the presence of hydrogen peroxide and nitrite, metMb nitrates exogenous tyrosine residues, although no mechanistic detail concerning the active species involved in these reactions is known.[10,16–18] These reactions are of great interest because the presence of ni-

[a] Dr. S. Nicolis, Dr. E. Monzani, Dr. R. Roncone, Prof. Dr. L. Casella
Dipartimento di Chimica Generale, Università di Pavia
27100 Pavia (Italy)
Fax: (+39) 0382-528544
E-mail: bioinorg@unipv.it

[b] Dr. L. Gianelli
Centro Grandi Strumenti, Università di Pavia, 27100 Pavia (Italy)

 DOI: 10.1002/chem.200304989

trated proteins is often observed under pathophysiological conditions.[19–22] A few potential nitrating agents have been recognized in vivo,[19] but the delineation of other biochemical pathways responsible for biological nitration and the identification of specific protein targets for nitration are essential for a full understanding of the mechanisms of NO•-derived pathologies.[23] Since during inflammatory diseases the levels of hydrogen peroxide and nitrite are markedly increased in cells,[24–26] heme proteins can use these components to produce nitrating agents. The ability of peroxidases to promote these reactions is well known.[18,23,27] In view of the much larger amount of Mb in the body, it is important to assess the possible role and significance of the nitrating activity of myoglobin in the presence of NO_2^-/H_2O_2. We have found that the metMb/NO_2^-/H_2O_2 system serves to nitrate exogenous phenolic compounds according to two limiting mechanisms, depending on nitrite concentration. The substrates are nitrated when they are bound to the protein, but the endogenous tyrosine residue (Tyr146) located in the proximal side of the protein is also competitively nitrated. This study provides an additional contribution to our understanding of the toxicity associated with increased expression and/or activity of NO synthases. The tyrosine derivatives **1**–**3** were chosen as representative substrates in the present investigation.

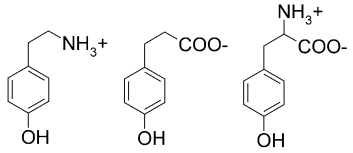

1 **2** **3**

Results

Binding of nitrite to metMb: Upon addition of nitrite, the Soret band of metMb shifts from 410 nm to 412 nm, characteristic of the $MbFe^{III}$–NO_2^- complex,[17] in which the nitrite anion binds to the iron as a nitro group through the nitrogen atom. From the dependence of the absorbance changes on the ligand concentration, the binding constant $K_B = (51 \pm 5)\,M^{-1}$ was obtained. The binding experiments were performed with short incubation times for the anion, since in the presence of high nitrite concentrations the Mb solution slowly turns a brownish-green color due to a modification of the heme.[28] The value of the binding constant obtained here is consistent with those extrapolated from kinetic studies ($K_B = K_D^{-1} = 81\,M^{-1}$ obtained at 20 °C in phosphate buffer at pH 7.5;[17] $K_B = 60\,M^{-1}$ obtained at 20 °C in Tris buffer at pH 7.4).[29]

Phenol nitration catalyzed by Mb: In the presence of hydrogen peroxide, metMb catalyzes the oxidative dimerization of phenols in a peroxidase-like reaction[30,31] involving the formation of phenoxy radicals. If the solution contains nitrite, nitrophenols are also produced.[16–18] The mechanism of this reaction was investigated by studying the nitration of substrates **1–3** by the metMb/H_2O_2/NO_2^- system. At pH 7.5, the nitrophenols are partially deprotonated and absorb at around 420 nm. To reduce the interference from the protein absorption during the kinetic experiments, the nitration reactions were followed by monitoring the increase of absorbance at 450 nm. In preliminary experiments, the rate of phenol nitration was studied as a function of metMb concentration, as well as by varying the NO_2^-, H_2O_2, and phenol concentrations to assess whether the nitration reaction in the absence of metMb, which can occur under acidic conditions,[32] would be likely to affect the kinetic data at pH 7.5. Since at a protein concentration of 1 μM the noncatalytic reaction could always be neglected, the kinetic experiments were performed with [metMb] fixed at this value. Each reactant was found to affect the observed rates in a manner dependent on the concentrations of the others. To simplify the analysis, it was found convenient to vary the concentration of one reagent while keeping the concentrations of the others fixed at the values found to maximize the rate. Plots of rate versus substrate concentration and of rate versus nitrite concentration showed saturation behavior, suggesting that both reactants have to interact with the protein. Figure 1 shows the dependence of the nitration rate of phenol **1** on [PhOH] (Figure 1A; where PhOH denotes in this contribution the appropriately substituted phenol) and [NO_2^-] (Figure 1B).

Nitration of the phenol can occur through several pathways. By reaction with hydrogen peroxide, metMb (simply indicated as Mb in the equations) forms an active species, $^{\bullet}MbFe^{IV}{=}O$, similar to the peroxidase compound I, with a radical localized on the protein backbone, which bears tyrosine and tryptophan residues.[35] This intermediate, either by spontaneous decay or after reaction with a substrate molecule, is transformed into an $MbFe^{IV}{=}O$ derivative similar to the peroxidase compound II. Both intermediates are able to react with nitrite, producing $NO_2^{\bullet}$, or with phenols, producing a phenoxy radical (PhO•), by one-electron oxidation. The phenoxy radical and $NO_2^{\bullet}$ can undergo a fast recombination reaction producing the nitrophenol. On the other hand, PhO• can also be produced by reaction of nitrogen dioxide with the phenol. If PhO• accumulates in solution, phenol coupling dimers can be produced.[30,31] This whole mechanism, denoted herein as path *a*, thus consists of the reactions (1)–(12).

$$Mb + H_2O_2 \rightarrow {}^{\bullet}MbFe^{IV}{=}O + H_2O \quad (1)$$

$${}^{\bullet}MbFe^{IV}{=}O + NO_2^- \rightleftharpoons [{}^{\bullet}MbFe^{IV}{=}O/NO_2^-] \quad (2)$$

$$[{}^{\bullet}MbFe^{IV}{=}O/NO_2^-] \rightarrow MbFe^{IV}{=}O + NO_2^{\bullet} \quad (3)$$

$${}^{\bullet}MbFe^{IV}{=}O + PhOH \rightleftharpoons [{}^{\bullet}MbFe^{IV}{=}O/PhOH] \quad (4)$$

$$[{}^{\bullet}MbFe^{IV}{=}O/PhOH] \rightarrow MbFe^{IV}{=}O + PhO^{\bullet} \quad (5)$$

$$MbFe^{IV}{=}O + NO_2^- \rightleftharpoons [MbFe^{IV}{=}O/NO_2^-] \quad (6)$$

$$[MbFe^{IV}{=}O/NO_2^-] + 2\,H^+ \rightarrow Mb + NO_2^{\bullet} + H_2O \quad (7)$$

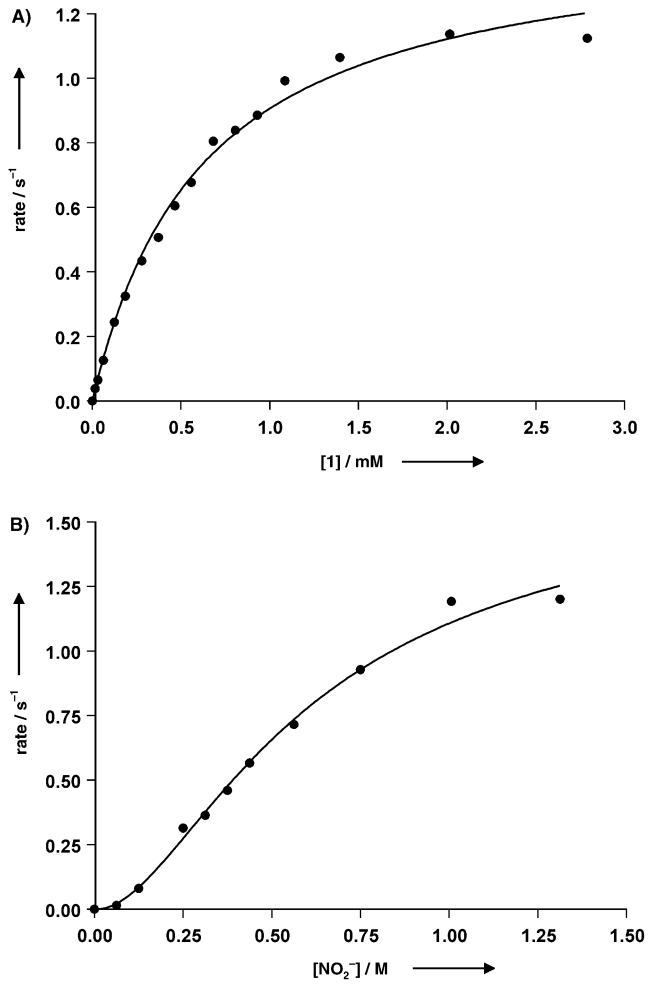

Figure 1. Dependence of the nitration rate of **1** on: A) phenol concentration, with $[NO_2^-] = 1.33$ M, and B) nitrite concentration, with [**1**] = 2.0 mM, at 25 °C in 0.2 M phosphate buffer, pH 7.5. The concentrations [metMb] = 1 μM and $[H_2O_2] = 0.37$ M were used.

$$MbFe^{IV}{=}O + PhOH \rightleftharpoons [MbFe^{IV}{=}O/PhOH] \quad (8)$$

$$[MbFe^{IV}{=}O/PhOH] + 2\,H^+ \rightarrow Mb + PhO^{\cdot} + H_2O \quad (9)$$

$$NO_2^{\cdot} + PhOH \rightarrow PhO^{\cdot} + NO_2^- \quad (10)$$

$$NO_2^{\cdot} + PhO^{\cdot} \rightarrow O_2N{-}C_6H_4{-}OH \quad (11)$$

$$2\,PhO^{\cdot} \rightarrow \text{dimers} \quad (12)$$

Here, [$^{\cdot}MbFe^{IV}{=}O/NO_2^-$], [$^{\cdot}MbFe^{IV}{=}O/PhOH$], [$MbFe^{IV}{=}O/NO_2^-$], and [$MbFe^{IV}{=}O/PhOH$] represent the complexes between nitrite or the phenol and the Mb active species, and $O_2N{-}C_6H_4{-}OH$ is the *ortho*-nitrophenol product. These protein complexes are believed to involve noncovalent interactions between nitrite or the phenol and the Mb derivative. In the case of metMb/PhOH complexes, the binding site of the phenol has been located near the heme periphery by NMR methods.[31] $^{\cdot}MbFe^{IV}{=}O$ can then react according to reactions (2)/(3) or (4)/(5) depending on $[NO_2^-]$, [PhOH], and the relative rate constants for the two processes; the same holds true for $MbFe^{IV}{=}O$, which can react through reactions (6)/(7) or (8)/(9). In any case, the nitrating agent in path *a* is assumed to be $NO_2^{\cdot}$.

In a different path, denoted herein as path *b*, it is considered that nitrite can bind directly to the iron(III) center of metMb. This complex then reacts with hydrogen peroxide producing a nitrating species that is able to nitrate a molecule of protein-bound phenol. Path *b* involves reactions (13)–(16):

$$Mb + NO_2^- \rightleftharpoons Mb{-}NO_2^- \quad (13)$$

$$Mb{-}NO_2^- + H_2O_2 \rightarrow Mb_{nitr} + H_2O \quad (14)$$

$$Mb_{nitr} + PhOH \rightleftharpoons [Mb_{nitr}/PhOH] \quad (15)$$

$$[Mb_{nitr}/PhOH] \rightarrow Mb + O_2N{-}C_6H_4{-}OH \quad (16)$$

Here, $Mb{-}NO_2^-$ is the nitrite complex of metmyoglobin, Mb_{nitr} represents an active nitrating form of the protein, which we assume to contain an iron-bound peroxynitrite, and [Mb_{nitr}/PhOH] is the complex between the latter species and the phenol. Path *b* differs from path *a* in that it is assumed that the mechanism does not involve peroxidase-like intermediates and nitrogen dioxide.

A detailed kinetic study of the nitration process is complicated by the number of steps and, therefore, the large number of binding constants and rate constants involved. Moreover, paths *a* and *b* could both be operative at the same time, thus implying several protein forms being simultaneously present in solution and the need to consider all of the reactions (1)–(16). A simplified analysis can be carried out by employing conditions under which one path predominates, assuming that the binding and dissociation processes are fast, and with a saturating hydrogen peroxide concentration. With these approximations, both the paths lead to the following initial rate equation (17),

$$\text{rate} = \frac{k_{cat}[Mb]}{1 + \dfrac{K^M_{nitrite}}{[NO_2^-]} + \dfrac{K^M_{PhOH}}{[PhOH]}} \quad (17)$$

where [Mb] is the total Mb concentration and k_{cat} represents the maximum turnover number of the protein. The meanings of $K^M_{nitrite}$ and K^M_{PhOH} relate to the mechanism involved, and give an indication of the dissociation constants for loss of NO_2^- and PhOH, respectively, from the complexes with the Mb form that are involved in each path. Equation (17) can be further simplified by operating under saturating conditions in terms of one of the two substrates; at high nitrite concentration, Equation (17) is reduced to Equation (18).

$$\text{rate} = \frac{k_{cat}[Mb][PhOH]}{K^M_{PhOH} + [PhOH]} \quad (18)$$

At high phenol concentration, Equation (19) is obtained.

$$\text{rate} = \frac{k_{cat}[Mb][NO_2^-]}{K^M_{nitrite} + [NO_2^-]} \quad (19)$$

The rate dependence on substrate concentration for phenols **1**–**3** (at high peroxide and nitrite concentrations) was found to be well interpolated by Equation (18). The values of k_{cat}, K^{M}_{PhOH}, and k_{cat}/K^{M}_{PhOH} thus obtained are reported in Table 1. The rate dependence on nitrite concentration for substrates **1**–**3** (at high peroxide and phenol concentrations) was interpolated by Equation (19). While for phenols **2** and **3** the interpolation was in good agreement with the experimental data, with tyramine (**1**) a biphasic behavior was observed (Figure 1B) since at low nitrite concentration the nitration rate was lower than the interpolated value. The values of k_{cat}, $K^{M}_{nitrite}$, and $k_{cat}/K^{M}_{nitrite}$ obtained are reported in Table 1; in the case of tyramine the reported values were obtained neglecting the data at low $[NO_2^-]$.

Table 1. Steady-state kinetic parameters for the metmyoglobin-dependent phenol nitration by NO_2^-/H_2O_2 in 0.2 M phosphate buffer pH 7.5 at 25 °C.

Phenol	K^{M}_{PhOH} [mM]	k_{cat} [s^{-1}]	k_{cat}/K^{M}_{PhOH} [$M^{-1}s^{-1}$]	$K^{M}_{nitrite}$ [M]	k_{cat} [s^{-1}]	$k_{cat}/K^{M}_{nitrite}$ [$M^{-1}s^{-1}$]
1	0.62 ± 0.05	1.47 ± 0.04	2400 ± 100	~0.6	~1.2	~2
2	0.14 ± 0.03	0.76 ± 0.03	5300 ± 800	0.14 ± 0.03	0.9 ± 0.1	6.9 ± 0.9
3	0.21 ± 0.02	0.69 ± 0.04	3300 ± 200	0.08 ± 0.02	0.43 ± 0.04	5 ± 1

Stopped-flow experiments: Several protein intermediates are involved in the phenol nitration reaction with the metMb/NO_2^-/H_2O_2 system. The prevalent protein species in solution depends on several factors, in particular on the kinetic parameters of the various reaction steps and the concentrations of the substrates. In the presence of 25 mM nitrite (a sub-saturating concentration for the turnover measurements, see Table 1), the Mb Soret band was slightly shifted from that of metMb (410 nm) due to partial coordination of the nitrite. Upon addition of 0.25 M peroxide (in the presence or absence of phenol **2**) the Soret band shifted to 424 nm (Figure 2, trace c), producing the same spectrum as that obtained on mixing metMb and peroxide. This indicates that the compound II-like intermediate was formed. In the presence of excess **2**, the nitrophenol optical band developed with time.

When the same experiments as above were performed in the presence of a higher nitrite concentration (250 mM; an almost saturating concentration for the turnover measurements, see Table 1), a different behavior was observed. In the absence of peroxide and **2**, the Mb Soret band appears at 412 nm (Figure 2, trace a), characteristic of the nitro complex of the protein. Upon addition of 0.25 M peroxide, the band shifts to 416 nm (Figure 2, trace b), while in the visible region optical absorptions are observed at 506, 538, 582 (sh), and 630 nm (sh) (Figure 2, trace d), with a pattern that differs significantly from both that of the Mb–NO_2^- complex and that of the $MbFe^{IV}$=O intermediate. The spectrum remains similar on increasing the peroxide concentration (up to 0.5 M), indicating that the 416 nm band does not result from an overlap of the bands due to two species. When the experiment was repeated in the presence of **2**, the same band at 416 nm was observed, the only difference being that the absorption of the nitrophenol produced by the reaction developed rapidly with time.

Inhibition effect of nitrite: A discriminating feature between path *a* and path *b* is the nitrite binding step. According to path *a*, the anion interacts with the protein after the reaction of metMb with the peroxide has taken place (reactions (2) and (6)). Coordination of NO_2^- to the metal would therefore reduce the rate of formation of the active species by competing with peroxide. The effect of nitrite can be easily studied at low peroxide concentration, conditions under which a reduction of the rate is to be expected on increasing the ni-

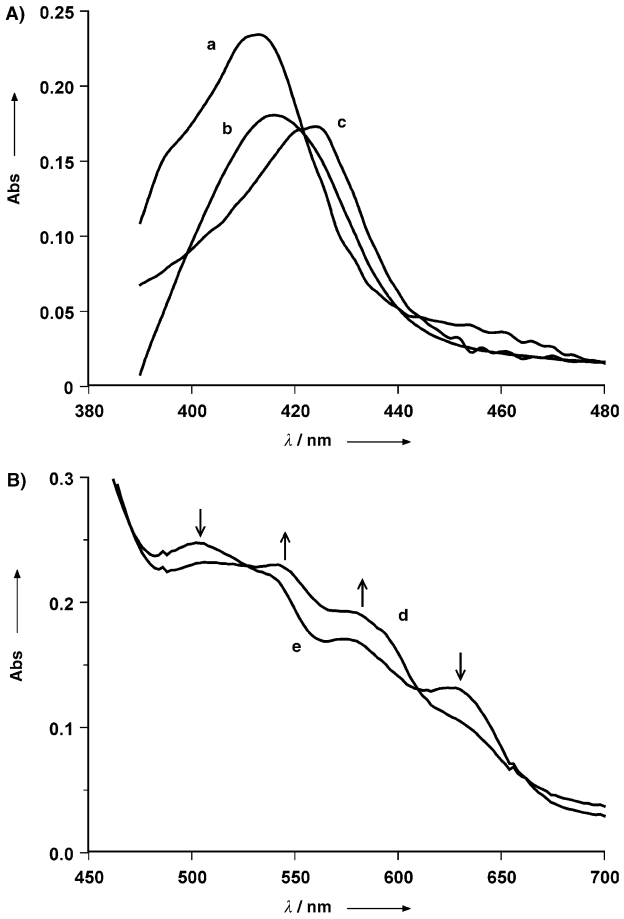

Figure 2. UV/Vis spectra of Mb forms observed in the stopped-flow experiments in the presence of various reagents, in 0.2 M phosphate buffer, pH 7.5, at 25 °C: A) trace a: Mb–NO_2^-; trace b: $MbFe^{III}$–N(O)OO; trace c: $MbFe^{IV}$=O. The concentration of metMb was 2.5 μM in all these experiments; those of the other reagents were as follows: a) $[NO_2^-]$ = 250 mM, [**2**] = 0.3 mM; b) $[NO_2^-]$ = 250 mM, [**2**] = 0.3 mM, $[H_2O_2]$ = 0.25 M; c) $[NO_2^-]$ = 25 mM, [**2**] = 0.3 mM, $[H_2O_2]$ = 0.25 M. The high nitrite concentration hinders the observation of the spectral range below 390 nm for traces a and b. B) trace d: $MbFe^{III}$–N(O)OO; trace e: Mb–NO_2^-. The concentration of metMb was 25 μM; those of the other reagents were as follows: d) $[NO_2^-]$ = 250 mM, [**2**] = 0.3 mM, $[H_2O_2]$ = 0.25 M; e) $[NO_2^-]$ = 250 mM, [**2**] = 0.3 mM. Blank spectra were obtained from mixtures of all the reagents with the exclusion of metMb. In all the experiments carried out in the presence of hydrogen peroxide, intense absorptions due to the phenol nitration products developed within a few seconds after mixing of the reagents. The reported spectra were therefore obtained within 1 s.

trite concentration. In path *b*, binding of NO_2^- to the iron precedes the reaction with peroxide. Therefore, at low peroxide concentration (when reaction according to Equation (14) is a slow step) an increase of nitrite concentration should enhance the rate according to the pre-equilibrium step [Eq. (13)].

Experiments aimed at investigating the effect of NO_2^- were carried out by varying the nitrite concentration (from 0.03 to 1.0 M) with a saturating concentration of **2** and keeping the peroxide concentration fixed at 4 mM. This value was chosen because the reaction rates depend linearly on $[H_2O_2]$ in the 0–5 mM range, indicating that in this range the reaction with the oxidant is the slow step of the cycle. The observed rates are plotted against $[NO_2^-]$ in Figure 3. The plot

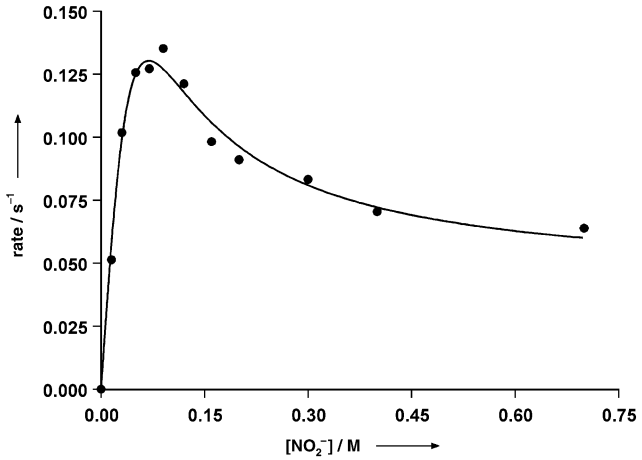

Figure 3. Dependence of the nitration rate of **2** on nitrite concentration at 25 °C in 0.2 M phosphate buffer, pH 7.5, with [metMb] = 1 μM, [**2**] = 1 mM, and $[H_2O_2]$ = 4 mM.

shows an initial increase at very low nitrite concentrations, which is consistent with both the paths since nitrite is necessary for the reaction. When the anion concentration exceeds 0.1 M, a reduction of the rate occurs, but the nitrophenol formation is not blocked even at $[NO_2^-]$ up to the molar range. This residual activity is not due to the noncatalytic reaction, because in the absence of metMb the rate is negligible. These observations imply that path *a* cannot be the only mechanism of the reaction, and are consistent with the involvement of path *b*.

Reaction of $MbFe^{IV}$=O with nitrite and phenols: The reduction of $MbFe^{IV}$=O by nitrite, **1**, or **2** was followed spectrophotometrically through monitoring the shift of the Soret band from 420 to 410–412 nm under pseudo-first-order conditions. In the case of nitrite, the observed first-order rate constants were found to be linearly dependent on nitrite concentration (Figure 4) according to Equation (20),

$$k_{obs} = k_{nitrite}[NO_2^-] + B \quad (20)$$

where the rate constant $k_{nitrite}$ probably consists of binding and reaction constants, since the overall process involves both reactions (6) and (7). The non-zero value of the intercept on the *y* axis is probably due to self-reduction of $MbFe^{IV}$=O to the met form or to heme-protein cross-linked forms.[17] Fitting of the experimental data to Equation (20) gave $k_{nitrite} = (18.6 \pm 0.6)\ M^{-1}s^{-1}$, in good agreement with the data reported by Herold and Rehmann ($16 \pm 1\ M^{-1}s^{-1}$, obtained at 20 °C).[17]

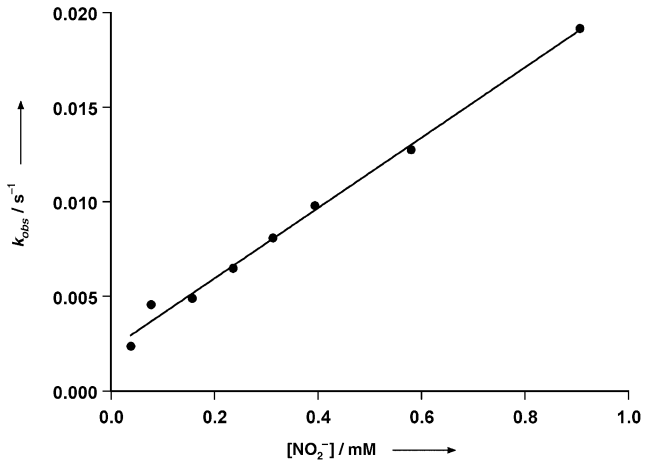

Figure 4. Dependence of the pseudo-first-order rate constant for reduction of $MbFe^{IV}$=O by nitrite on the concentration of this anion in 0.2 M phosphate buffer, pH 7.5, at 25 °C.

The spectral changes accompanying the reduction of $MbFe^{IV}$=O with an excess of phenol **1** of phenol **2** also followed a first-order behavior with time (data not shown). The observed first-order rate constants depend on the substrate concentration with a saturating behavior (Figure 5), which can be described by Equation (21),

$$k_{obs} = \frac{k_{cat,S}[PhOH]}{K_{M,S} + [PhOH]} + C \quad (21)$$

where $K_{M,S}$ represents the dissociation constant of the $MbFe^{IV}$=O/PhOH complex, and $k_{cat,S}$ is the first-order rate constant for decay of the complex to the iron(III) form. To take into account the self-decay of the compound II-like in-

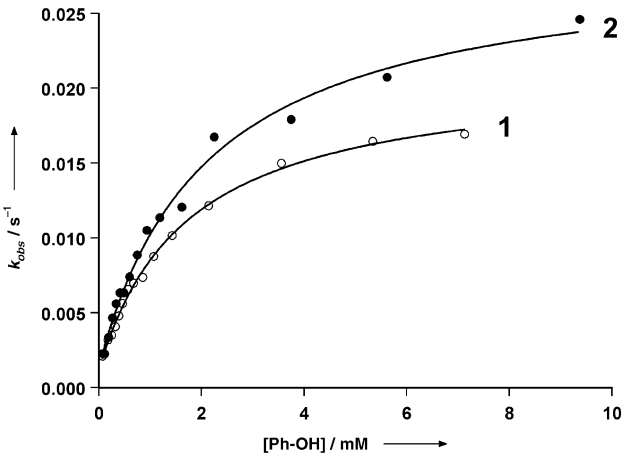

Figure 5. Dependence of the pseudo-first-order rate constants for reduction of $MbFe^{IV}$=O by **1** and **2** on the concentrations of these phenols in 0.2 M phosphate buffer, pH 7.5, at 25 °C.

termediate, the constant C has to be introduced into Equation (21). Fitting of the data plotted in Figure 5 with Equation (21) gave the kinetic parameters reported in Table 2.

Nitration of myoglobin: The nitrating species produced in the metMb/NO_2^-/H_2O_2 system could, in principle, react with endogenous tyrosine and tryptophan residues as well. The

Table 2. Kinetic parameters for $MbFe^{IV}$=O reduction by **1** and **2** in 0.2 M phosphate buffer at pH 7.5 at 25 °C.

Phenol	$K_{M,S}$ [mM]	$k_{cat,S}$ [s^{-1}]	$k_{cat,S}/K_{M,S}$ [$M^{-1}s^{-1}$]
1	1.7 ± 0.1	0.020 ± 0.001	11.6 ± 0.6
2	2.1 ± 0.3	0.026 ± 0.001	13 ± 1

porphyrin could also undergo nitration, and in fact it has been shown that upon treating the protein at pH 5.5 with a large excess nitrite, nitration of the heme vinyl groups occurs.[28] To assess whether metMb/NO_2^-/H_2O_2 can modify protein residues, HPLC/MS studies were carried out. A blank experiment was conducted with a small amount of metMb solution in 50 mM phosphate buffer, pH 7.5, which was directly injected into the HPLC/MS instrument. In view of the strong absorption of the heme near 410 nm, this was chosen as the working wavelength for UV detection. The resulting HPLC-UV chromatogram showed a peak at 42.5 min (data not shown), with a corresponding MS peak at *m*/*z* 616 attributable to free hemin. It would thus appear that the injected Mb is denatured in the HPLC column, and that hemin is released and separated from the apoprotein. In a separate experiment, metMb was treated under similar conditions as above, but with excess nitrite and hydrogen peroxide at 20 °C for 10 min, during which the color of the solution turned to greenish-brown and the Soret band was red-shifted. The solution was then dialyzed to remove excess peroxide and nitrite, and injected into the HPLC/MS instrument. The new chromatogram (Figure 6A) showed, besides the peak due to free hemin, a new peak at around 40.3 min, resulting from hemin nitration. The corresponding mass spectrum at this retention time gave an ion at *m*/*z* 661, 45 mass units above that of hemin and corresponding to the replacement of a proton in the porphyrin by NO_2. Assuming an equal sensitivity of the method for detection of the two porphyrins, integration of the peaks indicated that the nitration had occurred to an extent of nearly 33 %. When the same experiment was repeated with a higher hydrogen peroxide concentration (1 mM) added to the initial metMb solution containing nitrite, the production of nitrated hemin increased to about 50 % (Figure 6B). This indicates that the extent of nitration depends on the amount of oxidant added to the reaction mixture. Finally, Mb nitration was studied under the latter conditions (1 mM H_2O_2), but in the presence of 1 mM phenol **2**. The HPLC peak at 40.3 min also appeared in the presence of this phenol (Figure 6C), but the amount of nitrated hemin dropped to 14 %.

The possibility of nitration of protein residues by metMb/NO_2^-/H_2O_2 was assessed by subjecting a sample of the protein, previously incubated with 0.8 M NO_2^- and 1 mM H_2O_2,

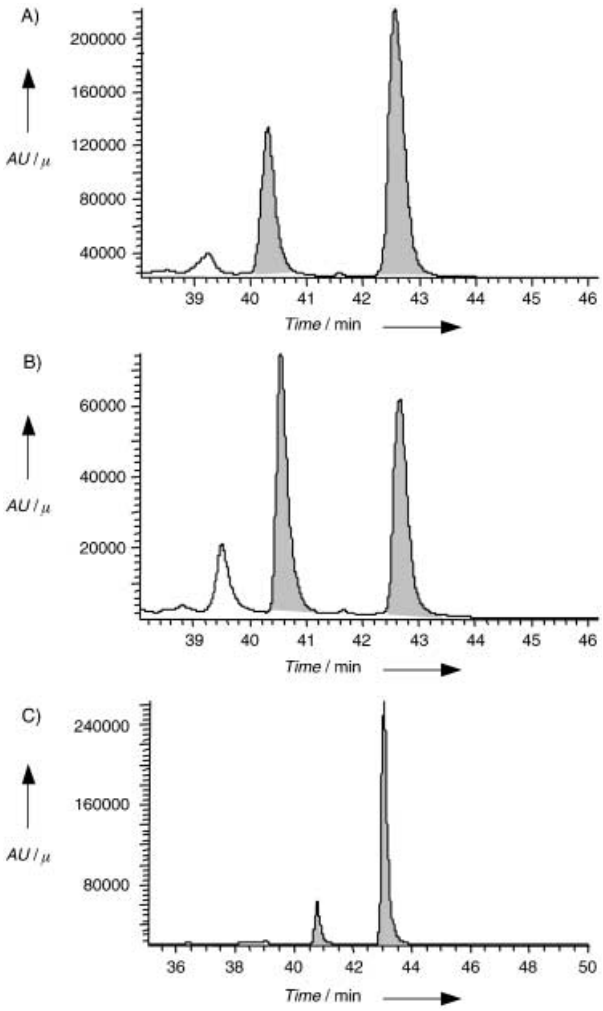

Figure 6. HPLC chromatograms, with detection at 410 nm, of metMb incubated in 50 mM phosphate buffer, pH 7.5, at 25 °C with 0.8 M nitrite and the following reagents: A) [H_2O_2] = 0.1 mM; B) [H_2O_2] = 1 mM; C) [H_2O_2] = 1 mM and [**2**] = 1 mM.

to a standard hydrochloric acid/2-butanone treatment. The apoprotein was isolated and subsequently digested by trypsin. The location of the nitration site was established by HPLC-MS/MS analysis of the tryptic fragments of the protein, by comparison with those obtained from digestion of untreated metMb under the same conditions. Data-dependent scan analysis was performed and the resulting data were treated with TurboSEQUEST for protein identification. TurboSEQUEST recognized Mb as the main protein present in the injected solution. A very high score was obtained and, with both native and modified (i.e. nitrated) myoglobin, all the peptides corresponding to the non-nitrated form of the protein were found in the chromatographic run.

Myoglobin contains four target amino acids for nitration (Tyr103, Tyr146, Trp7, and Trp14). The tryptic fragments containing such amino acids correspond to residues 1–16, 103–118, and 146–153 (the last one generated by a missing cleavage). Under the same conditions as used for the heme analysis, the elution times of the three unmodified peptides were 31.2, 36.7, and 20.6 min, respectively. For the metMb sample treated with H_2O_2/NO_2^- we analyzed the single-ion

currents of both the nitrated and standard peptides. In addition to the peaks due to non-nitrated fragments, the chromatogram showed a new peak with an elution time of 23.1 min corresponding to *m/z* 986. This molecular mass corresponds to that of the protein fragment 146–153 increased by 45 mass units, which corresponds exactly to the replacement of a proton by an NO_2 group. To confirm that this peak corresponds to nitration of a tyrosine residue, the MS/MS spectrum obtained was compared with the MS/MS spectrum of standard residue 146–153 (data not shown). The sequence of peptide 146–153 is YKELGFQG, with tyrosine as the N-terminal amino acid. A shift of 45 mass units was noted for all the ions containing the (N-terminal) Tyr residue, while the ions that first lost the (C-terminal) tyrosine were unchanged. This unambiguously identifies the nitration site as the aromatic ring of Tyr146.

To quantify the amount of nitrated tyrosine, a selected ion monitoring experiment was performed on the ions with *m/z* 941 and *m/z* 986. The single-ion chromatograms of the two characteristic ions allowed calculation of the area ratio of the two peaks. This indicated that the nitration of Tyr146 had occurred to an extent of about 6%. No detectable nitration peaks were found corresponding to Mb residues Tyr103, Trp7, and Trp14 in the fragments of the nitrated sample.

Discussion

In several diseases, particularly those connected with oxidative stress, an increased level of 3-nitrotyrosine is found.[19] A few mechanisms and nitrating agents have been proposed as being responsible for nitration. Nitration of tyrosine can occur through coupling of a tyrosyl radical with $NO^{\bullet}$, followed by oxidation of the resulting nitrosotyrosine. The nitrating agent can also be $NO_2^{\bullet}$, generated by oxidation of nitrogen monoxide or produced according to reactions (3) and (7). Other nitrating agents are nitrous acid, produced from nitrite at acidic pH, and peroxynitrite. The latter species, a strong nitrating agent, has a very short lifetime but is continuously produced in vivo by the reaction of $NO^{\bullet}$ with superoxide anion.[36,37] Further nitrating species can be produced by the oxidation of nitrite with hydrogen peroxide, although this reaction is usually negligible when the reagents are present at physiological concentrations. Peroxidases can catalyze the latter process, since they can produce both nitrogen dioxide and tyrosyl radicals, and these species can then couple to form nitrotyrosine.[38] The relative importance of the various pathways depends on the concentration of the enzymes and the $NO^{\bullet}$-derived species in the physiological fluids, particularly under oxidative stress conditions, under which hydrogen peroxide can be accumulated.[39]

Myoglobin is particularly abundant in tissues, where it can be present at concentrations of up to 0.2 mM.[11] It has been shown that MbO_2 can react with $NO^{\bullet}$ producing a protein-bound peroxynitrite,[9] and that $MbFe^{IV}{=}O$ is able to oxidize nitrite to $NO_2^{\bullet}$, and phenols to phenoxy radicals. Thus, Mb is a potential source of nitrotyrosine in the body, especially when the levels of nitrite and hydrogen peroxide are high. In spite of the level of importance that these processes may assume in vivo, no detailed investigation has been reported on the metMb/H_2O_2/NO_2^- system. Herold et al.[17] suggested that phenol nitration induced by the latter system is due to nitrogen dioxide formed by the reaction of $^{\bullet}MbFe^{IV}{=}O$ and $MbFe^{IV}{=}O$ species with nitrite. A different mechanism may, however, also be operative. In fact, it is known that nitrite in the protonated form readily reacts with hydrogen peroxide producing peroxynitrite.[40] In a similar manner, coordination of nitrite to the iron(III) center of metMb could also promote its reactivity towards H_2O_2, facilitating the formation of a bound peroxynitrite species.

We have considered the possible operation of two nitration mechanisms, indicated as path *a* (reactions (1)–(12)) and path *b* (reactions (13)–(16)), which differ in terms of the active species involved, namely $NO_2^{\bullet}$ and a protein-bound peroxynitrite, respectively. The analysis of the process is facilitated by monitoring the predominant form of the protein present in solution during turnover because this is related to the slow step of the catalytic cycle. According to path *a*, operating under saturating peroxide concentration (fast reaction with H_2O_2) and considering that $^{\bullet}MbFe^{IV}{=}O$ is a highly reactive species, the protein species accumulated during turnover should be $MbFe^{IV}{=}O$. With path *b*, under the same conditions, however, the predominant protein species should be the active nitrating species (Mb_{nitr}). The spectra of the protein intermediates recorded under various reaction conditions revealed the presence of different species depending on the nitrite concentration. At low nitrite concentration, the $MbFe^{IV}{=}O$ intermediate (λ_{max} = 424 nm) was observed, whereas at high nitrite concentration, a species with λ_{max} = 416 nm was observed. The spectrum of the latter differs from that of Mb–NO_2^-, and we suggest that it is due to heme-bound peroxynitrite. The spectrum of this species also differs from that of the peroxynitrite complex of Mb obtained from MbO_2 and $NO^{\bullet}$ (for which the Soret band is at 410 nm, and the pattern of bands in the visible region is also appreciably different).[10] This suggests that peroxynitrite is bound to the iron in different modes in the two complexes: through the peroxide oxygen, $MbFe^{III}$–OONO, when generated from MbO_2, and through the nitrogen atom, $MbFe^{III}$–N(O)OO, in the present case, where it is generated from Mb–NO_2^-. Arnold and Bohle[41] reported a UV/Vis spectrum, attributed to an intermediate $MbFe^{III}$–N(O)OO species, which was predicted from kinetic calculations on the singular value decomposition based on the spectral data obtained during the transformation of MbFeNO into metMb upon reaction with molecular oxygen. The absorption maxima resulting from those calculations differ from those obtained experimentally in this work; however, a closer look at the calculated spectrum reported by Arnold and Bohle shows that the intermediate is actually characterized by a broad Soret band with a maximum at 410 nm and a pronounced shoulder at low energy,[41] suggesting that the spectral features attributed to MbN(O)OO are mixed with those of the metMb form of the protein. The visible part of the spectrum for the proposed MbN(O)OO species reported by Arnold and Bohle also supports this hypothesis, since it shows only minor differences with respect to the metMb

spectrum[41] in the same region (between 520 and 600 nm); the MbN(O)OO spectrum obtained here differs strongly from that of metMb in this region (Figure 2).

The inhibition effect of nitrite at low peroxide concentration (Figure 3) confirms that $NO_2^{\bullet}$ cannot be the only nitrating species, since the reaction rates are not reduced to zero even at very high NO_2^- concentration, at which this anion might be expected to effectively compete with H_2O_2 for the binding sites at iron. The complex behavior revealed by the rate *versus* nitrite concentration plot is due to the fact that changing $[NO_2^-]$ has two effects: it changes the fraction of the protein bound to the ligand, and also the relative importance of paths *a* and *b*. This accounts for the differences in $K^M_{nitrite}$ values obtained for the different substrates. Path *b* is predominant at high $[NO_2^-]$; thus, k_{cat} represents the turnover number of the protein along this path. The similarity in k_{cat} values for reactions with phenols with different redox properties[42] indicates the high redox potential of the nitrating agent, as expected for a peroxynitrite-type active species. The k_{cat}/K^M_{PhOH} and K^M_{PhOH} parameters (obtained at saturating nitrite concentration) also relate to path *b*. In contrast, $k_{cat}/K^M_{nitrite}$ (the second-order rate constant for the reaction of nitrite with the $MbFe^{IV}$=O) gives the dependence of the reaction rates on nitrite at low anion concentration, conditions under which path *a* is dominant. The rate constants obtained for the reduction of $MbFe^{IV}$=O by NO_2^- or the phenolic substrates indicate that at the concentrations of the reactants used in the turnover experiments, the $MbFe^{IV}$=O intermediate invariably reacts with nitrite in preference to the phenol. Thus, reactions (6) and (7) are important steps in path *a*. Moreover, considering that $^{\bullet}MbFe^{IV}$=O is more reactive than $MbFe^{IV}$=O, the dependence of the turnover rate on nitrite in Equation (19) can be ascribed to reactions (6) and (7). According to this observation, $k_{cat}/K^M_{nitrite}$ can be compared with the second-order rate constant, $k_{nitrite}$, from Equation (20). The data in Table 1 show that the values of $k_{cat}/K^M_{nitrite}$ and $k_{nitrite}$ ($18.6 \pm 0.6\,M^{-1}s^{-1}$) are of the same order; the smaller values of the former parameter for all the substrates can be ascribed to the fact that a fraction of the protein is engaged in nonproductive nitrate formation.

To obtain an appreciation of the physiological relevance of paths *a* and *b*, the reactivity of metMb according to the two paths needs to be evaluated considering the concentration of the various species in the body, in particular during inflammatory processes whereby increased levels of H_2O_2 and nitrite are observed. Under such conditions, the hydrogen peroxide concentration can be of the order of 30 μM while that of nitrite can be up to 100 μM.[38] The latter value indicates that in vivo metMb is prevalently not coordinated by nitrite and this limits the contribution of the peroxynitrite mechanism. Nevertheless, during oxidative stress an increased concentration of nitrogen monoxide is produced in cells; under these conditions $MbFe^{IV}$=O reacts with $NO^{\bullet}$ at a rate ($k = (17.9 \pm 0.5) \times 10^6\,M^{-1}s^{-1}$ at pH 7.5)[17] which is much faster than the production of $NO_2^{\bullet}$ by reaction of $MbFe^{IV}$=O with nitrite ($k_{nitrite} = (18.6 \pm 0.6)\,M^{-1}s^{-1}$ at pH 7.5). Therefore, in vivo, path *a* is quenched and the metMb/H_2O_2/NO_2^- system contributes to phenol nitration only through path *b*.

The high intracellular Mb concentration[11] makes this protein a putative source of multiple nitrating species in the body. In its oxy form, Mb reacts with $NO^{\bullet}$ generating an Mb-bound peroxynitrite; in the $^{\bullet}MbFe^{IV}$=O and $MbFe^{IV}$=O forms it reacts with nitrite producing $NO_2^{\bullet}$; and in the met form it reacts with nitrite and hydrogen peroxide generating a highly reactive nitrating agent (peroxynitrite).

The nitrating species produced by the metMb/H_2O_2/NO_2^- system can also react with endogenous residues, in particular the heme prosthetic group, and the Tyr103, Tyr146, Trp7, and Trp14 residues. Our experiments indicate that both the porphyrin and Tyr146 undergo nitration. The extent of the modification increases with increasing peroxide concentration. Phenolic substrates protect the Mb from self-nitration. This last observation allows us to assume that our kinetic data are only related to the native protein and are not influenced by the fraction of Mb that may be competitively modified during catalysis, particularly since initial rates are considered. It is important to note that there is evidence of nitration only at Tyr146, while Tyr103 remains unaffected. This is somewhat surprising considering that the latter residue is exposed to solvent and the former is an internal residue (Figure 7). Therefore, the nitrating agent responsible for

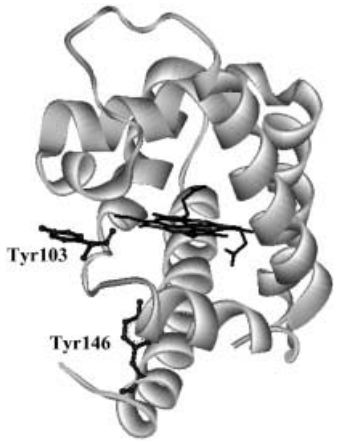

Figure 7. Structure of Mb showing the disposition of the side chains of Tyr103 and Tyr146.

self-nitration of Mb does not come from outside of the protein, but rather the reaction is intramolecular. This result is in keeping with the mechanisms of nitration of **1**–**3**, which show that only the protein-bound substrate is efficiently nitrated by the metMb/H_2O_2/NO_2^- system. It can be noted that Tyr146 is located in proximity to the Xe1 cavity of myoglobin;[43,44] this suggests that once the nitrating species (i.e. $NO_2^{\bullet}$ or $ONOO^-$) is produced close to the heme, it diffuses to the Xe1 cavity, where it performs the reaction on the Tyr146 residue. Our data differ from the results of Bourassa et al.,[13] who found that direct treatment of metMb with peroxynitrite led to nitration only at Tyr103. This difference may be due to the fact that in the experiment of Bourassa et al.[13] nitration of the exposed tyrosine occurs by reaction with free peroxynitrite or, perhaps less probably, that migration of the negatively charged $ONOO^-$ species to the Xe1

cavity is hindered. Interestingly, Herold et al.[15] reported that free peroxynitrite is scavenged by metMb whilst apoMb is nitrated only at Tyr146; this seems to indicate that exogenously supplied peroxynitrite is able to react at Tyr146 only where this residue is likely to be more exposed.

Experimental Section

Materials: Horse heart Mb was obtained from Sigma as a lyophilized sample and purified by gel permeation chromatography on a Sephadex G25 column with 100 mM phosphate buffer, pH 7.5, as eluent. Hydrogen peroxide (30 % (w/w) solution in water), tyramine (**1**), 3-(4-hydroxyphenyl)propionic acid (**2**), and L-tyrosine (**3**) were obtained from Aldrich. The other reagents were obtained at the best grade available. All buffer solutions were prepared by using doubly distilled deionized water. The concentrations of hydrogen peroxide solutions were determined by monitoring the formation of the ABTS radical cation according to a standard method.[45] The concentrations of myoglobin solutions were determined on the basis of the extinction coefficient of metMb, $1.88\times10^5\,M^{-1}cm^{-1}$, at 408 nm in 100 mM phosphate buffer, pH 6.0.[1] UV/Vis spectra were recorded on a Hewlett Packard HP 8452 A diode-array spectrophotometer.

Binding of nitrite: A concentrated nitrite solution in 200 mM phosphate buffer, pH 7.5, was added incrementally to a solution of metMb (3 μM, 1600 μL) in the same buffer (final concentration from 0.012 to 0.31 M) thermostatted at 25.0 ± 0.1 °C in a quartz cuvette with optical pathlength 1 cm, and UV/Vis spectra were recorded after each addition. Blank spectra were recorded in the same way but in the absence of the protein. After subtracting the corresponding blank from each spectrum, the resulting spectra were corrected for dilution and then transformed into difference spectra by subtracting the native protein spectrum. The absorbance changes at 422 nm, the wavelength of maximum change in the difference spectra, were then plotted against the ligand concentration. The binding constant, K_B, was obtained by interpolation of the absorbance data with the binding isotherm for low affinity binding of a single ligand: $\Delta A = \Delta A_\infty K_B[NO_2^-]_{tot}/(1+K_B\times[NO_2^-]_{tot})$, where $[NO_2^-]_{tot}$ represents the total nitrite concentration in the optical cell.

Kinetic studies: All kinetic experiments were carried out by spectrophotometric monitoring of solutions in 200 mM phosphate buffer at pH 7.5 in a quartz cuvette of pathlength 1 cm, thermostatted at 25.0 ± 0.1 °C and equipped with a magnetic stirrer.

Phenol nitration catalyzed by metMb: The reactions were studied by monitoring the absorbance change at 450 nm during the first 10–15 s after adding an H_2O_2 solution to a metMb/substrate/nitrite solution (final volume 1600 μL), obtained by mixing concentrated solutions of the reactants in 200 mM phosphate buffer at pH 7.5. The pH values of the mother nitrite and phenol solutions in the buffer were adjusted to the above value by adding sodium hydroxide or phosphoric acid. The rate data were transformed from absorbance s^{-1} into $[nitrophenol]_{produced}\,s^{-1}$ on the basis of the extinction coefficients of the nitrophenols at 450 nm obtained from their absorbance spectra[46] in phosphate buffer at pH 7.5: for **1**, $\varepsilon_{450\ nm} = 2300$; for **2**, $\varepsilon_{450\ nm} = 3350$; for **3**, $\varepsilon_{450\ nm} = 3100\,M^{-1}cm^{-1}$. Kinetic parameters were obtained from fitting of the experimental rates at different substrate/nitrite concentrations to the appropriate equations.

For each substrate, the rate dependence on the various reactant concentrations was studied by applying the following series of steps: 1) determination of the peroxide concentration that maximizes the reaction rate with saturating substrate and nitrite concentrations (typically starting from [phenol] = 1 mM and $[NO_2^-]$ = 0.3 M); 2) study of the dependence of the rate on the substrate concentration while maintaining $[H_2O_2]$ as optimized in the previous step and $[NO_2^-]$ saturating; 3) study of the dependence of the rate on the nitrite concentration, maintaining $[H_2O_2]$ as found in step 2 and [PhOH] saturating; 4) if the substrate and nitrite concentrations that maximize the rate did not fit with those used in step 1, the whole procedure was repeated starting with different $[NO_2^-]$ and [phenol] in an iterative way. The metMb concentration was kept at 1 μM in all the reactions and the concentrations of the other reactants used in the kinetic studies were as follows: 1) for optimization of the peroxide concentration, substrate **1**: [PhOH] = 1.0 mM, $[NO_2^-]$ = 1.33 M, $[H_2O_2]$ = 0.05–0.6 M; substrate **2**: [PhOH] = 0.31 mM, $[NO_2^-]$ = 0.30 M, $[H_2O_2]$ = 0.05–0.3 M; substrate **3**: [PhOH] = 0.55 mM, $[NO_2^-]$ = 0.30 M, $[H_2O_2]$ = 0.03–0.2 M; 2) dependence of the rate on the phenol concentration: substrate **1**: $[H_2O_2]$ = 0.37 M, $[NO_2^-]$ = 1.33 M, [PhOH] = 0.016–2.8 mM; substrate **2**: $[H_2O_2]$ = 0.30 M, $[NO_2^-]$ = 0.3 M, [PhOH] = 0.031–1.4 mM; substrate **3**: $[H_2O_2]$ = 0.16 M, $[NO_2^-]$ = 0.30 M, [PhOH] = 0.007–0.7 mM; 3) dependence of the rate on the nitrite concentration: substrate **1**: $[H_2O_2]$ = 0.37 M, [PhOH] = 2.00 mM, $[NO_2^-]$ = 0.063–1.3 M; substrate **2**: $[H_2O_2]$ = 0.30 M, [PhOH] = 0.78 mM, $[NO_2^-]$ = 0.062–0.63 M; substrate **3**: $[H_2O_2]$ = 0.16 M, [PhOH] = 0.78 mM, $[NO_2^-]$ = 0.012–0.19 M.

Dependence of the nitration rate of 2 on the nitrite concentration at low oxidant concentration: Kinetic experiments were carried out by standard methods with low $[H_2O_2]$, saturating [PhOH], and varying $[NO_2^-]$. The peroxide concentration was selected by studying the dependence of the reaction rate on $[H_2O_2]$; the concentrations of the reagents were as follows: [metMb] = 1 μM, [PhOH] = 1 mM, $[NO_2^-]$ = 0.1 M, and $[H_2O_2]$ = from 0.5 to 5.0 mM. The dependence of the nitration rate on the nitrite concentration was studied with the following reactant concentrations: [metMb] = 1 μM, [PhOH] = 1 mM, $[H_2O_2]$ = 4 mM, $[NO_2^-]$ = 0.03–1.0 M.

Stopped-flow experiments: The stopped-flow experiments were performed on a thermostatted Applied Photophysics RX-1000 instrument, with a dead time of 1 ms, equipped with two syringes (A and B) connected to a cuvette (optical pathlength 1 cm). Syringe A was filled with a solution of the protein, nitrite and, in some of the experiments, substrate **2**, in 200 mM phosphate buffer at pH 7.5, 25.0 ± 0.1 °C; syringe B was filled with an H_2O_2 solution in water or just water. Mixing of the solutions in the cuvette thus halved the reactant concentrations. Final concentrations of the reactants were: [metMb] = 2.5 μM, $[NO_2^-]$ = 25 mM in the low nitrite concentration experiments and $[NO_2^-]$ = 250 mM in the high nitrite concentration experiments, [PhOH] = 0.3 mM, and $[H_2O_2]$ = 0.25 M. Spectra were recorded in the visible region as above but using [metMb] = 25 μM. Absorbance spectra were recorded every 0.2 seconds for a total time of 10 seconds; blanks were recorded with nitrite solutions at the same concentrations as used in each experiment.

Reactions of $MbFe^{IV}$=O: The Mb compound II-like intermediate was prepared by incubating metMb (4 μM) with two equivalents of H_2O_2 for about 10 min, until the Soret band shifted from 410 nm to 420 nm and stabilized at this wavelength. Here, the incubation time should not be prolonged, because cross-linking of the protein can occur.[47] The reduction of $MbFe^{IV}$=O to metMb after the addition of nitrite (0.04–0.9 mM), phenol **1** (0.08–7.2 mM) or phenol **2** (0.07–9.4 mM) solutions was followed spectrophotometrically by recording the absorbance changes at 410 and 428 nm.

Nitration of Mb and analysis of protein fragments: Two samples of nitrated Mb were prepared by adding sodium nitrite (final concentration 0.8 M) and hydrogen peroxide (final concentration 0.1 mM or 1 mM) to metMb (10 mg) dissolved in 50 mM phosphate buffer at pH 7.5 (6 mL). The mixtures were allowed to react at 20 °C for 10 min; excess nitrite and oxidant were removed by transferring the samples into a dialysis membrane kept in a large vessel containing 10 mM phosphate buffer at pH 7.5 (500 mL) under slow stirring at 4 °C. Dialysis was continued overnight under these conditions with several changes of the buffer. Then, UV/Vis spectra of the nitrated myoglobins were recorded, and both samples were analyzed by HPLC/MS.

A portion of each sample was transformed into apoMb by standard hydrochloric acid/2-butanone treatment[1] and subsequently hydrolyzed by protease. Digestion was performed with 1:50 (w/w) trypsin at 36 °C for 2 h in 50 mM phosphate buffer at pH 7.5. The samples were then analyzed by HPLC/MS.

Protein nitration in the presence of a phenolic substrate was performed by adding nitrite (0.8 M), hydrogen peroxide (1 mM), and **2** (final concentration 1 mM) to metMb (10 mg) dissolved in the same buffer as above (6 mL); the sample was then treated according to the same procedure as described above.

An LCQ-DECA ion-trap mass spectrometer (Thermo-Finnigan) equipped with an electrospray ionization source was used to obtain the LC-MS and LC-MS/MS data. The ESI conditions were as follows: capillary temperature 250 °C, tube lens −25 V, source voltage +4.9 kV. The HPLC pump was a Spectra System P4000 and the UV/Vis detector was a Spectra System UV2000 working in double-wavelength mode (230 and

410 nm). HPLC analysis was carried out with a Hypersil Elite C18 column (250×4.6 mm, 5 μm). The solvents used were: solvent A: 0.1% trifluoroacetic acid (TFA) in distilled water, and solvent B: 0.1% TFA in CH_3CN; gradient runs were performed with a flow rate of 0.8 mL min^{-1}. The elution was performed by running for 2 min with 5% B, then with a gradient to 40% B over 48 min, and finally with a gradient to 0% B over 10 min. Nitrated residues were identified with the aid of TurboSEQUEST (from Thermo-Finnigan, San Jose, CA)[48] software, which allows the automatic identification of proteins by comparing tandem (MS/MS) mass spectra of the peptides obtained by tryptic degradation of Mb with predicted MS/MS spectra from a sequence database. Data-dependent scan analysis was coupled with the use of TurboSEQUEST. The procedure involves experiments in which the instrument repetitively records ESI-MS spectra in a chromatographic run and switches to MS/MS mode when a component elutes into the mass spectrometer. The system is capable of identifying the molecular ion and, in the following scan cycle, through MS/MS experiment, of detecting the fragmentation pattern of the selected ion.

Acknowledgements

This work was supported by the Italian MURST, through a PRIN Project, the Italian CNR, through the target project on "Biotechnology", and by the European INTAS and COST programmes. R. Roncone thanks the C.I.R.C.M.S.B. for financial support.

[1] E. Antonini, M. Brunori, *Hemoglobin and Myoglobin in their Reactions with Ligands*, North Holland, Amsterdam, The Netherlands, **1971**.
[2] L. Stryer, *Biochemistry*, W. H. Freeman & Co., New York, USA, **2002**.
[3] J. B. Wittenberg, B. A. Wittenberg, *Annu. Rev. Biophys. Chem.* **1990**, *19*, 217–241.
[4] S.-I. Ozaki, H.-J. Yang, T. Matsui, Y. Goto, Y. Watanabe, *Tetrahedron: Asymmetry* **1999**, *10*, 183–192.
[5] D. Galaris, E. Cadenas, P. Hochstein, *Arch. Biochem. Biophys.* **1989**, *273*, 497–504.
[6] M. Nakamura, S. Nakamura, *Biophys. Biochim. Acta* **1996**, *1289*, 329–335.
[7] B. A. Springer, S. G. Sligar, J. S. Olson, G. N. Phillips, *Chem. Rev.* **1994**, *94*, 699–714.
[8] J. K. Møller, L. J. Skibsted, *Chem. Rev.* **2002**, *102*, 1167–1178.
[9] S. Herold, *FEBS Lett.* **1999**, *443*, 81–84.
[10] S. Herold, M. Exner, T. Nauser, *Biochemistry* **2001**, *40*, 3385–3395.
[11] M. Brunori, *Trends Biochem. Sci.* **2001**, *26*, 21–23.
[12] M. Brunori, *Trends Biochem. Sci.* **2001**, *26*, 209–210.
[13] J. L. Bourassa, E. P. Ives, A. L. Marqueling, R. Shimanovich, J. T. Groves, *J. Am. Chem. Soc.* **2001**, *123*, 5142–5143.
[14] P. K. Witting, A. G. Mauk, D. J. Douglas, R. Stocker, *Biochem. Biophys. Res. Commun.* **2001**, *286*, 352–356.
[15] S. Herold, K. Shivashankar, M. Mehl, *Biochemistry* **2002**, *41*, 13460–13472.
[16] K. Kilinc, A. Kilinc, R. E. Wolf, M. B. Grisham, *Biochem. Biophys. Res. Commun.* **2001**, *285*, 273–276.
[17] S. Herold, F.-J. K. Rehmann, *J. Biol. Inorg. Chem.* **2001**, *6*, 543–555.
[18] L. Casella, E. Monzani, R. Roncone, S. Nicolis, A. Sala, A. De Riso, *Environ. Health Perspect.* **2002**, *110*, 709–711.
[19] H. Ischiropoulos, *Arch. Biochem. Biophys.* **1998**, *356*, 1–11.
[20] Q. W. Xie, C. Nathan, *J. Leukocyte Biol.* **1994**, *56*, 576–582.
[21] D. Saleh, P. J. Barnes, A. Giaid, *Am. J. Respir. Crit. Care Med.* **1997**, *155*, 1763–1769.
[22] B. Halliwell, *FEBS Lett.* **1997**, *411*, 157–160.
[23] I. V. Turko, F. Murad, *Pharmacol. Rev.* **2002**, *54*, 619–634.
[24] J. Hunt, R. E. Byrns, L. J. Ignarro, B. Gaston, *Lancet* **1995**, *346*, 1235–1236.
[25] D. Torre, G. Ferrario, F. Speranza, A. Orani, G. P. Fiori, C. Zeroli, *J. Clin. Pathol. (Lond.)* **1996**, *49*, 574–576.
[26] W. A. Pryor, G. L. Squadrito, *Am. J. Physiol.* **1995**, *268*, L699–L722.
[27] M.-L. Brennan, W. Wu, X. Fu, Z. Shen, W. Song, H. Frost, C. Vadseth, L. Narine, E. Lenkiewicz, M. T. Borchers, A. J. Lusis, J. J. Lee, N. A. Lee, H. M. Abu-Soud, H. Ischiropoulos, S. L. Hazen, *J. Biol. Chem.* **2002**, *277*, 17415–17427.
[28] L. L. Bondoc, R. Timkovic, *J. Biol. Chem.* **1989**, *264*, 6134–6145.
[29] A. Wanat, J. Gdula-Argasińska, D. Rutkowskazbik, M. Witko, G. Stokel, R. van Eldik, *J. Biol. Inorg. Chem.* **2002**, *7*, 165–176.
[30] E. Monzani, G. Alzuet, L. Casella, C. Redaelli, C. Bassani, A. M. Sanangelantoni, M. Gullotti, L. De Gioia, L. Santagostini, F. Chillemi, *Biochemistry* **2000**, *39*, 9571–9582.
[31] C. Redaelli, E. Monzani, L. Santagostini, L. Casella, A. M. Sanangelantoni, R. Pierattelli, L. Banci, *ChemBioChem* **2002**, *3*, 226–233.
[32] T. D. Oury, L. Tatro, A. J. Ghio, C. A. Piantadosi, *Free Radical Res.* **1995**, *23*, 537–547.
[33] M. J. Davies, *Free Radical Res. Commun.* **1990**, *10*, 361–370.
[34] J. J. O. Turner, C. A. Rice-Evans, M. J. Davies, E. S. R. Newman, *Biochem. Soc. Trans.* **1990**, *18*, 1056–1059.
[35] A. C. Onuoha, J. F. Rusling, *J. Am. Chem. Soc.* **1997**, *119*, 3979–3986.
[36] N. V. Blough, O. C. Zafiriou, *Inorg. Chem.* **1985**, *24*, 3502–3504.
[37] W. H. Koppenol, J. J. Moreno, W. A. Pryor, H. Ischiropoulos, J. S. Beckman, *Chem. Res. Toxicol.* **1992**, *5*, 834–842.
[38] A. Van der Vliet, J. P. Eiserich, B. Halliwell, C. E. Cross, *J. Biol. Chem.* **1997**, *272*, 7617–7625.
[39] J. K. Hurst, S. V. Lymar, *Acc. Chem. Res.* **1999**, *##32##35*, 520–528.
[40] M. N. Hughes, H. G. Nicklin, *J. Chem. Soc.* **1968**, 450–452.
[41] E. V. Arnold, D. S. Bohle, *Methods Enzymol.* **1996**, *269*, 41–55.
[42] E. Monzani, A. L. Gatti, A. Profumo, L. Casella, M. Gullotti, *Biochemistry* **1997**, *36*, 1918–1926.
[43] M. Brunori, Q. H. Gibson, *EMBO Reports* **2001**, *8*, 674–679.
[44] H. Frauenfelder, B. H. McMahon, R. H. Austin, K. Chu, J. T. Groves, *Proc. Natl. Acad. Sci. USA* **2001**, *98*, 2370–2374.
[45] L. Casella, L. De Gioia, G. Frontoso Silvestri, E. Monzani, C. Redaelli, R. Roncone, L. Santagostini, *J. Inorg. Biochem.* **2000**, *79*, 31–39.
[46] E. Monzani, R. Roncone, L. Casella, M. Galliano, W. H. Koppenol, unpublished data.
[47] Y. Osawa, K. Korzekwa, *Proc. Natl. Acad. Sci. USA* **1991**, *88*, 7081–7085.
[48] R. E. Moore, M. K. Young, T. D. Lee, *J. Am. Soc. Mass Spectrom.* **2002**, *13*, 378–386.

Received: March 25, 2003
Revised: December 1, 2003 [F4989]